TRANSPLANTATION

Ex vivo enzymatic treatment converts blood type A donor lungs into universal blood type lungs

Aizhou Wang[1], Rafaela V. P. Ribeiro[1], Aadil Ali[1], Edson Brambate[1], Etienne Abdelnour-Berchtold[1], Vinicius Michaelsen[1], Yu Zhang[1], Peter Rahfeld[2], Haisle Moon[3], Hemant Gokhale[1], Anajara Gazzalle[1], Prodipto Pal[4], Mingyao Liu[1,5], Thomas K. Waddell[1,6], Christine Cserti-Gazdewich[7], Kathryn Tinckam[4,8], Jayachandran N. Kizhakkedathu[3,9], Lori West[10,11], Shaf Keshavjee[1,6], Stephen G. Withers[2], Marcelo Cypel[1,6]*

Donor organ allocation is dependent on ABO matching, restricting the opportunity for some patients to receive a life-saving transplant. The enzymes FpGalNAc deacetylase and FpGalactosaminidase, used in combination, have been described to effectively convert group A (ABO-A) red blood cells (RBCs) to group O (ABO-O). Here, we study the safety and preclinical efficacy of using these enzymes to remove A antigen (A-Ag) from human donor lungs using ex vivo lung perfusion (EVLP). First, the ability of these enzymes to remove A-Ag in organ perfusate solutions was examined on five human ABO-A1 RBC samples and three human aortae after static incubation. The enzymes removed greater than 99 and 90% A-Ag from RBCs and aortae, respectively, at concentrations as low as 1 μg/ml. Eight ABO-A1 human lungs were then treated by EVLP. Baseline analyses of A-Ag in lungs revealed expression predominantly in the endothelial and epithelial cells. EVLP of lungs with enzyme-containing perfusate removed over 97% of endothelial A-Ag within 4 hours. No treatment-related acute lung toxicity was observed. An ABO-incompatible transplant was then simulated with an ex vivo model of antibody-mediated rejection using ABO-O plasma as the surrogate for the recipient circulation using three donor lungs. The treatment of donor lungs minimized antibody binding, complement deposition, and antibody-mediated injury as compared with control lungs. These results show that depletion of donor lung A-Ag can be achieved with EVLP treatment. This strategy has the potential to expand ABO-incompatible lung transplantation and lead to improvements in fairness of organ allocation.

INTRODUCTION

Lung transplantation is a life-saving therapy for end-stage lung diseases. Successful organ transplantation depends on using donor organs that display protein or carbohydrate antigens on their surface that are immunologically compatible with the recipient. If not matched, preexisting donor-specific antibodies present in the recipient's circulation will initiate rapid immune responses, which can lead to destruction of the graft and failure of the organ. Among the more critical antigens requiring compatibility are the A and B antigens, which are part of the ABO histo-blood group system. The need to match multiple antigens reduces the probability of finding a compatible donor, thereby increasing times on waitlists. This situation results in not only increased waitlist mortality for some patients but also wastage of donor organs that cannot be matched. For example, ABO-O candidates for lung transplantation generally have to wait longer and have a 20% greater risk of dying while awaiting an acceptable donor than do ABO-A, ABO-B, or ABO-AB individuals (*1*). Thus, any means to decrease matching requirements or effectively create "ABO-agnostic organs" would effectively expand the donor pool for such recipients and markedly improve the fairness and access to organ allocation.

A small subset of transplants, mostly kidneys, is performed in adults using organs from ABO-incompatible (ABOi) donors. The procedure is performed primarily with subgroup ABO-non-A1 donors (low A antigen expression) into ABO-O or ABO-B recipients (with low anti-A antibody titers) along with recipient desensitization protocols to minimize rejection (*2*). It has been observed that, although these patients may begin to produce ABO antibodies again after ABOi transplantation, graft injury often does not occur. This phenomenon, called "accommodation," is effected by mechanisms that remain incompletely understood (*3*, *4*). Although 5-year survival outcomes have been reported to be equivalent between ABOi versus ABO-compatible (ABOc) kidney transplants, higher early mortality and complications have been observed in patients who received the ABOi grafts. This is most likely due to the recipient-centric desensitization protocols: For instance, the oversuppressed immune system leads to higher risk of infectious complications, and repeated plasmapheresis procedures led to changes in the coagulation system and higher rates of bleeding events (*5*, *6*). In contrast to kidney transplantation, intentional ABOi transplant is not currently performed in lung transplantation. Therefore, a donor-centric antigen removal approach could be envisioned to decrease the burden of augmented immunosuppression on the recipient and to safely expand the practice of ABOi transplantation to all mismatch combinations, instead of just the current small subset.

[1]Latner Thoracic Surgery Research Laboratories, Ajmera Transplant Centre, Toronto General Hospital Research Institute, University Health Network, ON M5G 1L7, Canada. [2]Department of Chemistry, University of British Columbia, Vancouver, BC V6T 1Z1, Canada. [3]Centre for Blood Research, Department of Pathology and Laboratory Medicine, Life Science Institute, University of British Columbia, Vancouver, BC V6T 1Z3, Canada. [4]Department of Laboratory Medicine and Pathobiology, University of Toronto, ON M5S 1A8, Canada. [5]Departments of Surgery, Medicine and Physiology and Institute of Medical Science, Temerty Faculty of Medicine, University of Toronto, ON M5T 1P5, Canada. [6]Division of Thoracic Surgery, Department of Surgery, University of Toronto, Toronto, ON M5T 1P5, Canada. [7]Transfusion Medicine and Hematology, University Health Network, Toronto, ON M5G 2C4, Canada. [8]Department of Medicine, University Health Network and University of Toronto, Toronto, ON M5G 2C4, Canada. [9]School of Biomedical Engineering, University of British Columbia, Vancouver, BC V6T 1Z3, Canada. [10]Department of Pediatrics, University of Alberta, Edmonton, AB T6G 1C9, Canada. [11]Canadian Donation and Transplantation Research Program, Edmonton AB T6G 1C9, Canada.
*Corresponding author. Email: marcelo.cypel@uhn.ca

The ABH(O) antigens are oligosaccharides. The difference between A, B, and H antigens resides in whether an additional terminal sugar epitope (α-galactose or *N*-acetyl-galactosamine) is present on the nonimmunogenic H-oligosaccharide. Previous attempts to convert A or B antigens on red cells to H involved the use of α-*N*-acetyl-galactosaminidase or α-galactosidase enzymes, respectively (*7*). Rahfeld *et al.* (*8*) recently identified enzymes (FpGalNAc deacetylase and FpGalactosaminidase), hereafter called Azymes, that removes A antigen (A-Ag) with high specificity and efficiency. The authors demonstrated efficient conversion of whole units of ABO-A blood to ABO-O using Azymes. In the present study, we evaluate the early organ safety and preclinical efficacy of using Azymes to remove A-Ag from donor lungs during ex vivo lung perfusion (EVLP). The efficacy of Azymes was examined sequentially from in vitro cell- and tissue-based studies to ex vivo human whole-organ studies.

RESULTS

A-Ag is removed by Azymes in lung perfusate solution

The concept of enzymatic removal of ABO antigen is illustrated in Fig. 1A. The schematic overview of the study is illustrated in fig. S1. Azymes were previously tested in phosphate-buffered saline (PBS) and whole blood. Their ability to remove A-Ag in lung perfusate solution, which contains human serum albumin and dextran 40 as the key ingredients (*9*), was unknown. Here, we demonstrate that Azymes effectively remove A-Ag in lung perfusate solution at the dose range of 0.2 to 4 μg/ml when compared with PBS alone (Fig. 1B). In lung perfusate solution after 30 min of static treatment at 37°C, Azymes removed 44.5 ± 5.2% (0.2 μg/ml dose), 82.2 ± 4.7% (0.5 μg/ml dose), 95.3 ± 2.1% (1 μg/ml dose), and 100.00 ± 0.02% (4 μg/ml dose) A-Ag from RBCs. Azymes in lung perfusate solution achieved significantly higher ($P < 0.0001$) antigen removal at doses of 0.2, 0.5, and 1 μg/ml than in PBS (Fig. 1C), demonstrating the role of dextran, a component of the perfusate solution, in enhancing Azyme activity, as previously described (*10*).

Static treatment of human aortae with Azymes removes A-Ag

It was important to show the efficacy of Azymes in removing antigens from tissue before treating whole organs. Human aortae from organ donors were chosen as our initial tissue model and subjected to static treatment with Azyme-spiked perfusate solution (Fig. 1D). The dose of 1 μg/ml, at which over 90% removal of A-Ag was observed for RBCs, was chosen as the starting dose for aorta treatment, along with two additional higher doses of 2 and 5 μg/ml. A-Ag expression in aortae was observed primarily on endothelial cells, as staining for A-Ag colocalized with the endothelial marker, CD31 (Fig. 1E, control). Upon treatment with the Azymes, the positive staining of A-Ag was lost (Fig. 1E, treatment). Static treatment of aortae using Azymes (1 μg/ml) in perfusate solution resulted in removal of 92 ± 1% of A-Ag (Fig. 1F). Similar effects were seen at all three tested doses (1, 2, and 5 μg/ml), indicating that the lowest dose tested could be an effective dose for use in EVLP treatment.

A and H antigens are expressed in endothelia and epithelia of blood group A human lungs

Individuals of blood group A subdivide into subgroup A1 (80% of A population) and non-A1 (20% of A population), differing primarily in density of antigen expression. To treat histo-blood group antigens from whole organs, it is essential to understand the distribution and expression profile of the antigens in human lungs. We first used immunostaining to determine the location of A-Ag and found that it is expressed on lung endothelia and epithelia (Fig. 2A). A-Ag was observed on blood vessels (solid arrow, $CD31^+$) and airspaces (dashed arrow, $CD31^-$). To further elucidate the distribution and quantify the blood group antigens, we used flow cytometry to measure the expression of A and H antigens among four main types of pulmonary cells: endothelial cells, epithelial cells, alveolar macrophages, and leukocytes (Fig. 2B). Cells from both A1 ($n = 8$) and non-A1 ($n = 4$) donors were evaluated. Regardless of subgroup status, flow cytometric analysis revealed the expression of A-Ag primarily located on pulmonary endothelial and epithelial cells, corroborating our immunostaining results (Fig. 2A). In addition, we found that A1 individuals expressed significantly higher A-Ag on endothelial cells [median fluorescence intensity (MFI) = 29,130 ± 6054], almost 46 times higher MFI as compared with those in the non-A1 individuals (MFI = 638 ± 161, $P < 0.001$) (Fig. 2C, top). In the non-A1 samples, the pulmonary endothelial blood group antigens are mostly in the form of its precursor, the H antigen (Fig. 2C, bottom). The expression profile of histo-blood group A and H antigens on pulmonary endothelial cells from non-A1 individuals more closely resembles that of an ABO-O individual than an ABO-A1 individual (fig. S2). With this information, ABO-A1 lungs were used to study whole-organ treatment, as they are more prevalent and highly immunogenic to an ABOi recipient because of higher antigen expression.

A-Ag was depleted from human lungs by Azyme treatment using EVLP

Human lungs from multiorgan donors (ABO-A1, $n = 8$), determined to be unsuitable for clinical transplantation, were treated with Azymes using the Toronto EVLP protocol (fig. S3). The donor characteristics are summarized in Table 1. Different doses and treatment durations were tested for optimal treatment conditions. Within 1 hour of treatment, a marked vascular clearance of A-Ag was observed (Fig. 3A), accompanied by the appearance of H-Ag, consistent with the Azymes' proposed mechanism of action (Fig. 3B). A-Ag was depleted by over 97% under all three tested conditions. The 1-hour treatment with the 1 μg/ml dose led to 2.40 ± 0.05% ($n = 2$) remaining vascular A-Ag. The 3-hour treatment with the 1 μg/ml dose led to 2.43 ± 0.60% ($n = 5$, $P < 0.0001$ versus pretreatment) remaining vascular A-Ag. The 3-hour treatment with 5 μg/ml led to 2.53% ($n = 1$) remaining vascular A-Ag (Fig. 3C). A-Ag reduction was observed in lung epithelia as well (fig. S4). Considering that our treatment was delivered through perfusion, this observed reduction is likely due to leakiness of the rejected lungs and extravasation of Azymes. No acute side effects were observed in lung physiology (Fig. 3D). We also did not observe any differences in inflammatory cytokines (Fig. 3E) after initiation of the enzymatic treatment. These studies demonstrate that well within the usual time span of clinical EVLP (4 hours) (*9*), the Azymes at the lowest tested dose (1 μg/ml) were effective in achieving a high degree of A-Ag removal along the endothelia of perfused human lungs.

Simulation of ABOi lung transplant with a human EVLP reperfusion model

Having identified conditions for effective removal of A-Ag, we established an ex vivo plasma reperfusion model to simulate and

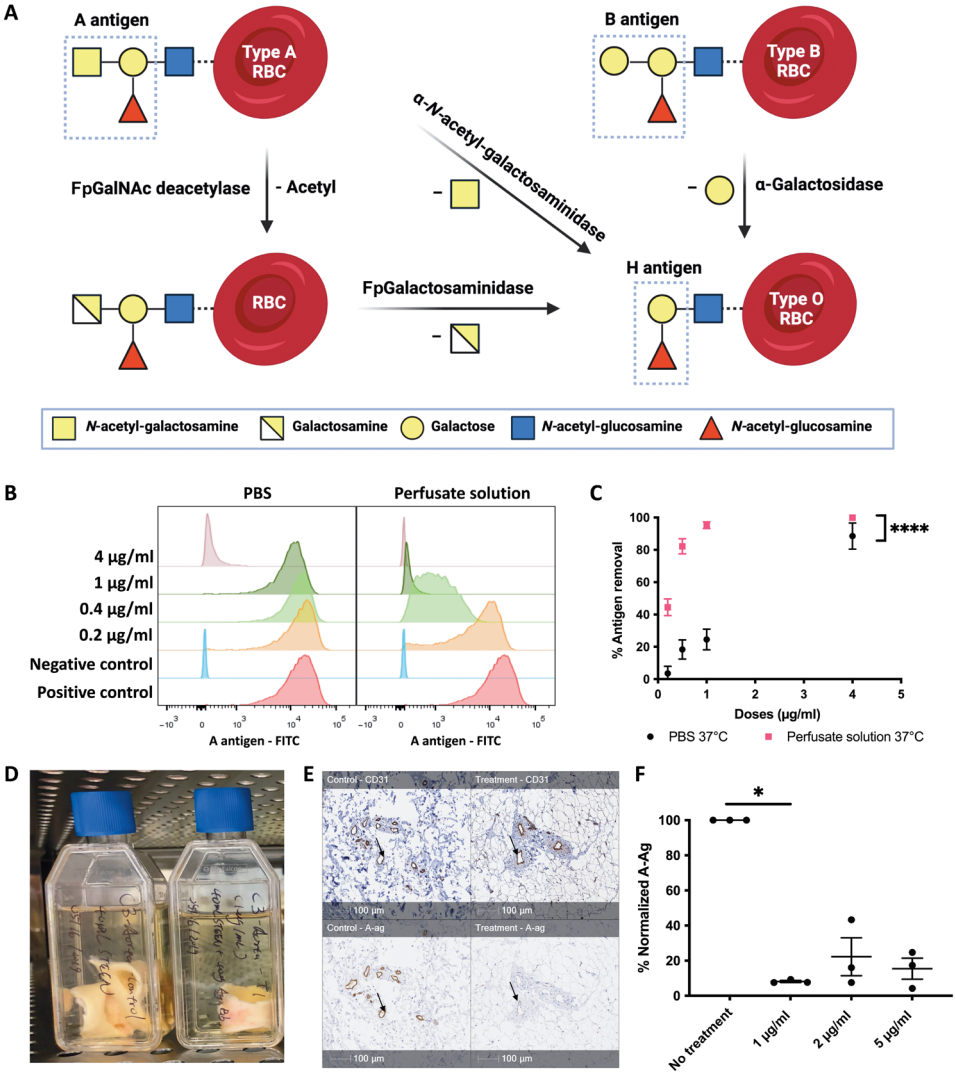

Fig. 1. Azymes removed A-Ag from human ABO-A1 RBCs and aortae in the presence of perfusate solution. (**A**) Concept of enzymatic removal of ABO antigen. The dashed boxes show basic ABH antigens on red blood cells (RBCs) [modified from Rahfeld *et al.* (*8*)]. Enzymatic reactions by respective enzymes remove the terminal α-*N*-acetyl-galactosamine or α-galactose monosaccharide and turn A/B red cells to an O type. This study examines the paired enzymatic actions by FpGalNAc deacetylase and FpGalactosaminidase (Azymes) to remove A antigen (A-Ag) from organs. Sugars are shown using the Consortium for Functional Glycomics (CFG) notation (*30*). (**B**) The histograms show A-Ag expression on RBCs treated with Azymes at the indicated doses in either PBS or perfusate solution. RBCs were treated for 30 min at 37°C. The positive control is untreated ABO-A RBCs, and the negative control is group ABO-O RBCs. Cells were stained with fluorescein isothiocyanate (FITC)–conjugated anti-A antibody. (**C**) The degree of antigen removal was quantified on the basis of percent changes in MFI relative to baseline. For each dose group, $n = 5$ RBC treatments were conducted. (**D**) The image shows static incubation of aortae in perfusate solution. Samples were incubated without (control) or with Azymes (treatment) at 37°C for 4 hours. (**E**) Representative images of immunohistochemical staining of aortae are shown, zoomed in the adventitial side. Positive staining is denoted by brown color and arrows. A-Ag staining colocalized with CD31 staining, which indicates endothelial cells, in control aortae, but was reduced after Azyme treatment. Scale bars, 100 μm. (**F**) The dose effect of Azymes on aortae was quantified on the basis of percent change in the abundance of A-Ag normalized to control aortae. Data in (C) and (F) are presented as means ± SEM. Data in (C) were analyzed using two-way analysis of variance (ANOVA) and Bonferroni's multiple comparisons test. ****$P < 0.0001$. Data in (F) were analyzed using Kruskal-Wallis test and Dunn's multiple comparisons test. *$P < 0.05$.

assess the effects of antigen depletion on preventing or alleviating antibody-mediated injuries in an ABOi transplant (Fig. 4A). Lungs from the same donor (hence with similar antigen expression) were split into left and right lungs and randomized as control or treatment. Plasma samples from ABO-O individuals, with necessary antibodies and complement, were used as the surrogate recipient circulation such that the addition of plasma to the EVLP system initiated the "reperfusion phase." Antibody-mediated injuries were assessed on the basis of changes in circulating anti-A antibodies, tissue-bound antibodies, complement, inflammatory cytokines, lung physiology, and lung histology.

X-ray images of the donor lungs before randomization are shown in fig. S5. The pulmonary endothelial A-Ag density and the concentrations of inflammatory cytokines in the paired control and treatment donor groups, and the antibody and complement characteristics of the "recipients" (ABO-O plasma) before reperfusion are summarized in Table 2 ($n = 3$). Consistent with our results in the EVLP studies, enzyme treatment of the lungs reduced the vascular expression of A-Ag to 2.4, 1.7, and 1.0%, respectively, when compared to baseline, whereas that of the control lungs remained high. In all three cases, depletion of vascular A-Ag effectively prevented antibody binding (Fig. 4, B to J). Upon addition of ABO-O plasma, the influx of circulating anti-A antibodies was rapidly depleted in the control groups because of absorption onto tissue surfaces, but remained stable in the treatment groups over the course of reperfusion (Fig. 4, B to D). Correspondingly, antibody was indeed shown to be adsorbed onto the endothelia of the control lung at the end of reperfusion (Fig. 4, E to G). Changes in the circulating and tissue-bound antibodies are summarized in Fig. 4 (H to J). At the end of reperfusion, changes in circulating complement factors were not significantly different between the two groups: C1q ($P = 0.13$), C3 ($P = 0.21$), and C3b ($P = 0.81$) (Fig. 4K). The control lungs from all three cases showed significantly higher concentrations of the inflammatory cytokines tumor necrosis factor–α (TNF-α) ($P = 0.040$) and interferon–γ (IFN-γ) ($P = 0.026$), comparing to the respective treatment lungs (Fig. 4L).

The upstream biological changes led to somewhat different degrees of downstream effects reflected in the lung physiology and histology in the three cases. In case 1, the control lung experienced an increase in peak airway pressure from 12 to 17 cmH_2O, whereas that of the treatment lung changed from 11 to 12 cmH_2O (Fig. 5A). The changes in dynamic lung compliance

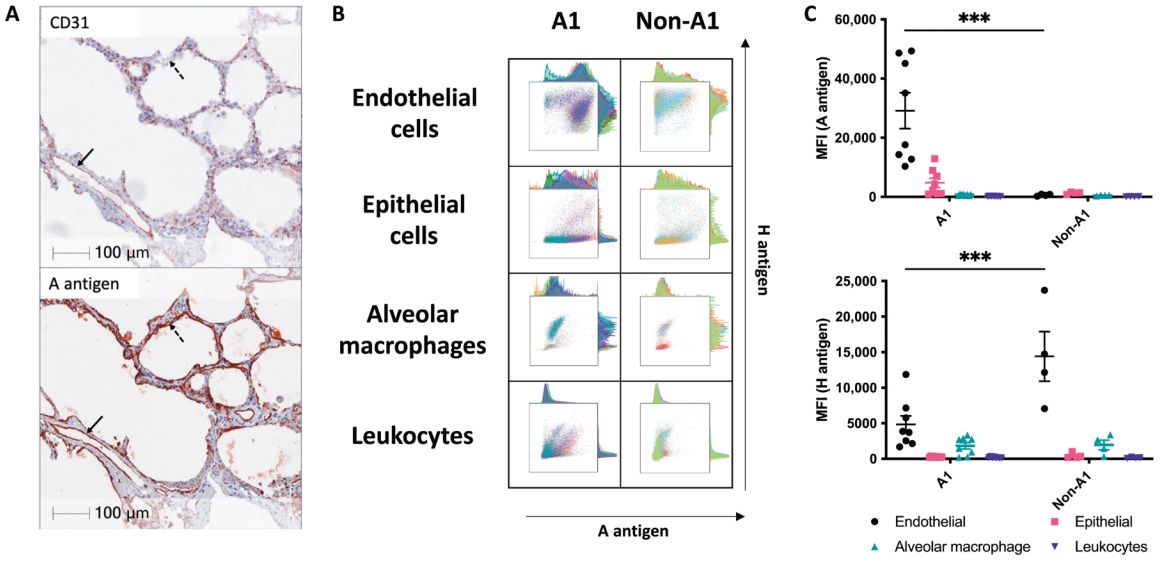

Fig. 2. ABH antigens are differentially expressed in blood group A1 and non-A1 human lungs. (**A**) Representative immunohistochemical images show expression of A-Ag on endothelium (solid arrow, CD31$^+$) and epithelium (dashed arrow, CD31$^-$) of lung tissue from an ABO-A1 donor. Scale bars, 100 μm. (**B**) Scatter plots show the expression of A and H antigens on different types of cells isolated from subgroup A1 ($n = 8$) or non-A1 ($n = 4$) donor lungs. (**C**) MFIs of A-Ag (top) are primarily observed in endothelial and epithelial cells of A1 donor, whereas H-Ag (bottom), the precursor of A-Ag, is seen on endothelial cells from both A1 and non-A1 lungs. Data in (C) are presented as means ± SEM. Data were analyzed using two-way ANOVA with Bonferroni's multiple comparisons test. ***$P < 0.001$.

Table 1. Donor information for lungs that received EVLP treatment. DCD, donation after cardiac death; NDD, neurological determination of death; F, female; M, male.

Donor no.	Age	Sex	Lungs treated	Paired control	DCD or NDD	Clinical EVLP before treatment (hours)	Treatment dose (μg/ml)	Treatment length (hours)
Treatment studies								
1	36	F	Right		NDD	4	1	1
2	78	M	Right		NDD	4	1	3
3	71	F	Right		DCD	4	5	3
4	28	M	Left	Right	NDD	0	1	3
5	63	M	Left		DCD	0	1	3
6	49	F	Right		DCD	0	1	3
Treatment + plasma reperfusion studies								
7	59	M	Right	Left	DCD	4	1	1
8	59	M	Right	Left	DCD	0	1	3
9	41	M	Right	Left	NDD	4	1	3

and PaO_2 were similar between the two lungs (Fig. 5, B and C). More edema was observed in the control lung as indicated by the increased wet-to-dry ratio (Fig. 5D). In case 2, the treated lung had stable physiology, whereas the control lung presented drastic deterioration (Fig. 5, E to H). In case 3, both the control and treatment lungs had stable physiology (Fig. 5, I to K) during reperfusion and low wet-to-dry ratio (Fig. 5L) despite the distinct pattern observed in antibody binding (Fig. 4, D to J). Similar trends to those observed in lung physiology were also observed in the tissue C4d deposition (Fig. 5M). The control lungs from the three cases had borderline positive, positive, and negative C4d staining, respectively, whereas all three treatment lungs had negative staining. No marked differences were observed in lung histology (Fig. 5, N and O) or terminal deoxynucleotidyl transferase–mediated deoxyuridine triphosphate nick end labeling–positive (TUNEL$^+$) cells, as a readout of apoptosis in the lung tissue (Fig. 5, P and Q).

DISCUSSION

Here, we present our strategy to overcome the ABO compatibility requirement in lung transplantation by converting A-Ag of donor lungs to H antigen using an EVLP treatment approach. By perfusing human donor lungs with specific Azymes (FpGalNAc deacetylase and FpGalNase) (*8*) that remove the A epitopes of *N*-acetyl galactosamine, we successfully converted ABO-A1 donor lungs to "universal" donor ABO-O lungs. Subsequent ABOi transplant simulation demonstrated

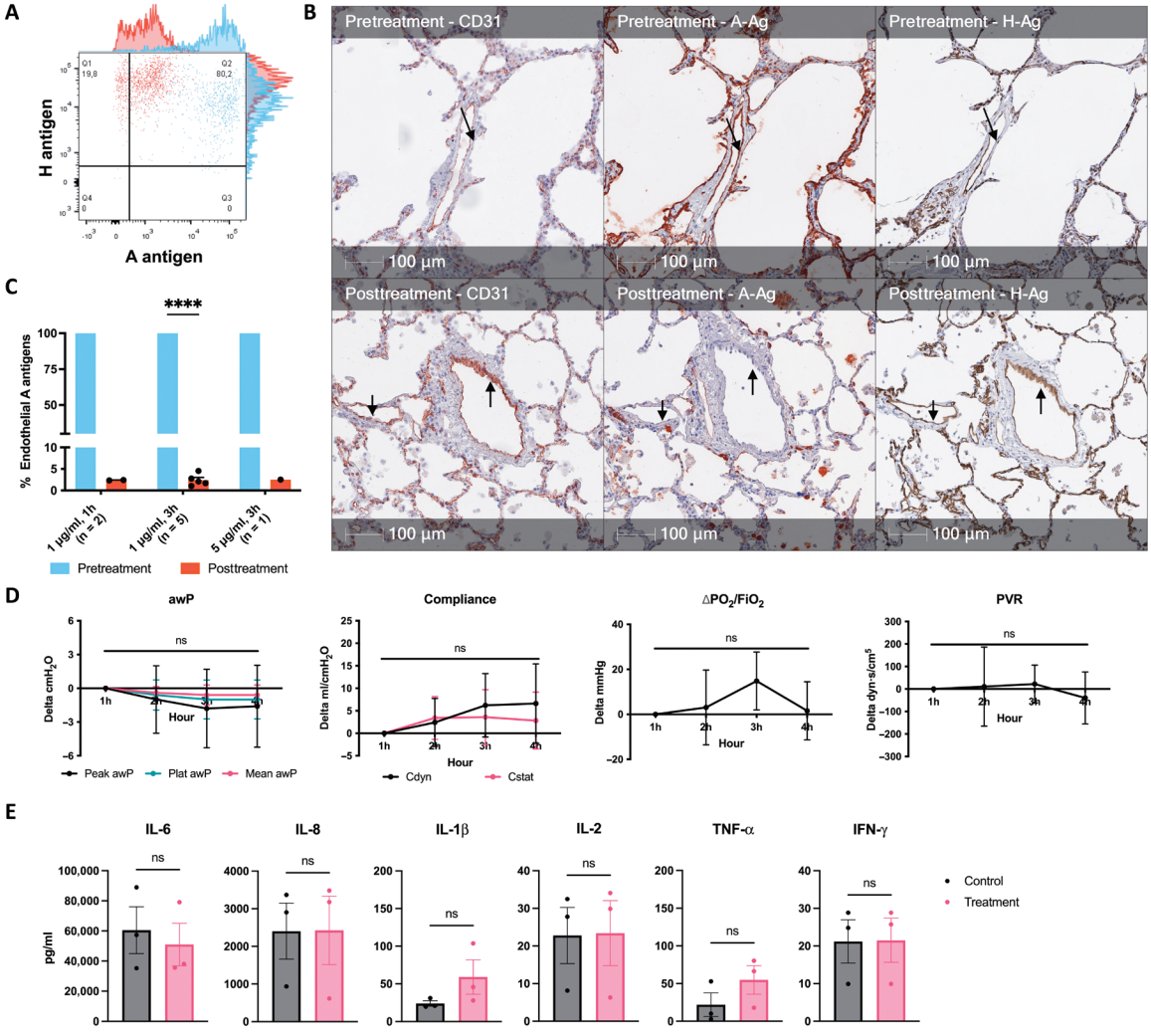

Fig. 3. Azymes removed A-Ag from perfused human lung. (**A**) Scatter plots are shown of A-Ag and precursor H-Ag expression on endothelial cells ($CD45^{-}CD31^{+}$) homogenized from human lungs that were treated with Azymes (1 μg/ml) for 1 hour; blue is pretreatment, and red is posttreatment. (**B**) Representative immunohistochemical images of lung before and after treatment with Azymes are shown. Positive staining is denoted by red color. Pretreatment, staining for both A-Ag and H-Ag, was observed on blood vessels. After treatment, vascular A-Ag staining was not observed, whereas H-Ag staining remained positive. Solid arrows denote CD31-expressing regions. Scale bars, 100 μm. (**C**) Effects of dose and treatment duration on depletion of endothelial A-Ag were quantified by MFI of A-Ag signal from $CD45^{-}CD31^{+}$ cells. The MFI of the pretreatment sample from each case was set to 100% to normalize the posttreatment A-Ag signals. The tested conditions include 1 μg/ml for 1 hour ($n = 2$), 1 μg/ml for 3 hours ($n = 5$), and 5 μg/ml for 3 hours ($n = 1$). Data in (C) were analyzed using two-way ANOVA and Bonferroni's multiple comparisons test. ****$P < 0.0001$. (**D**) No significant impairment was observed in parameters of lung function test after 3 hours of treatment at 1 μg/ml ($n = 5$), which was administered after assessment at hour 1 (1h) as baseline. Lung physiology was expressed as change from baseline to adjust for variability in quality among the human donor lungs declined for clinical transplantation. Peak awP, peak airway pressure; Plat awP, plateau airway pressure; Mean awP, mean airway pressure; Cdyn, dynamic compliance; Cstat, static compliance; $\Delta PO_2/FiO_2$, functional oxygenation; PVR, pulmonary vascular resistance. Data in (D) were analyzed using two-way ANOVA and Dunnett's multiple comparisons test. ns, not significant. (**E**) Inflammatory responses were measured in paired single lungs ($n = 3$ per group) receiving 3 hours of normal perfusion (control) versus Azyme treatment (1 μg/ml). Each pair of control and treatment was from the same donor. The concentration (pg/ml) shown on the graphs is the differences between the hour-4 cytokine (after 3 hours of treatment or normal perfusion) and hour-1 cytokine (before treatment or normal perfusion). Data in (E) were analyzed using paired *t* test. Data are presented as means ± SEM.

that the Azyme preconditioned lung was able to tolerate perfusion with plasma of an ABOi recipient, thus avoiding the early phases of antibody-mediated injury.

There are about 100,000 patients on U.S. organ transplant waiting lists (*11*). These patients require organs that must be compatible to their major cell surface antigens. The process to find compatible organs is not trivial. Because of this, patients with progressively failing organs often wait years for a life-saving transplant, and some will die, never receiving an optimally matched organ. In 2017, less than one-third of patients on the lung transplant waiting list received an organ in the United States (*11*). Specifically, access to an organ from an ABOc donor is inequitable among patients of the four major ABO phenotypes. Because organs from ABO-O donors are compatible with recipients of all blood groups, a recent report showed that ABO-O patients face a higher risk of dying while waiting for an acceptable lung allograft than do those of the other blood groups

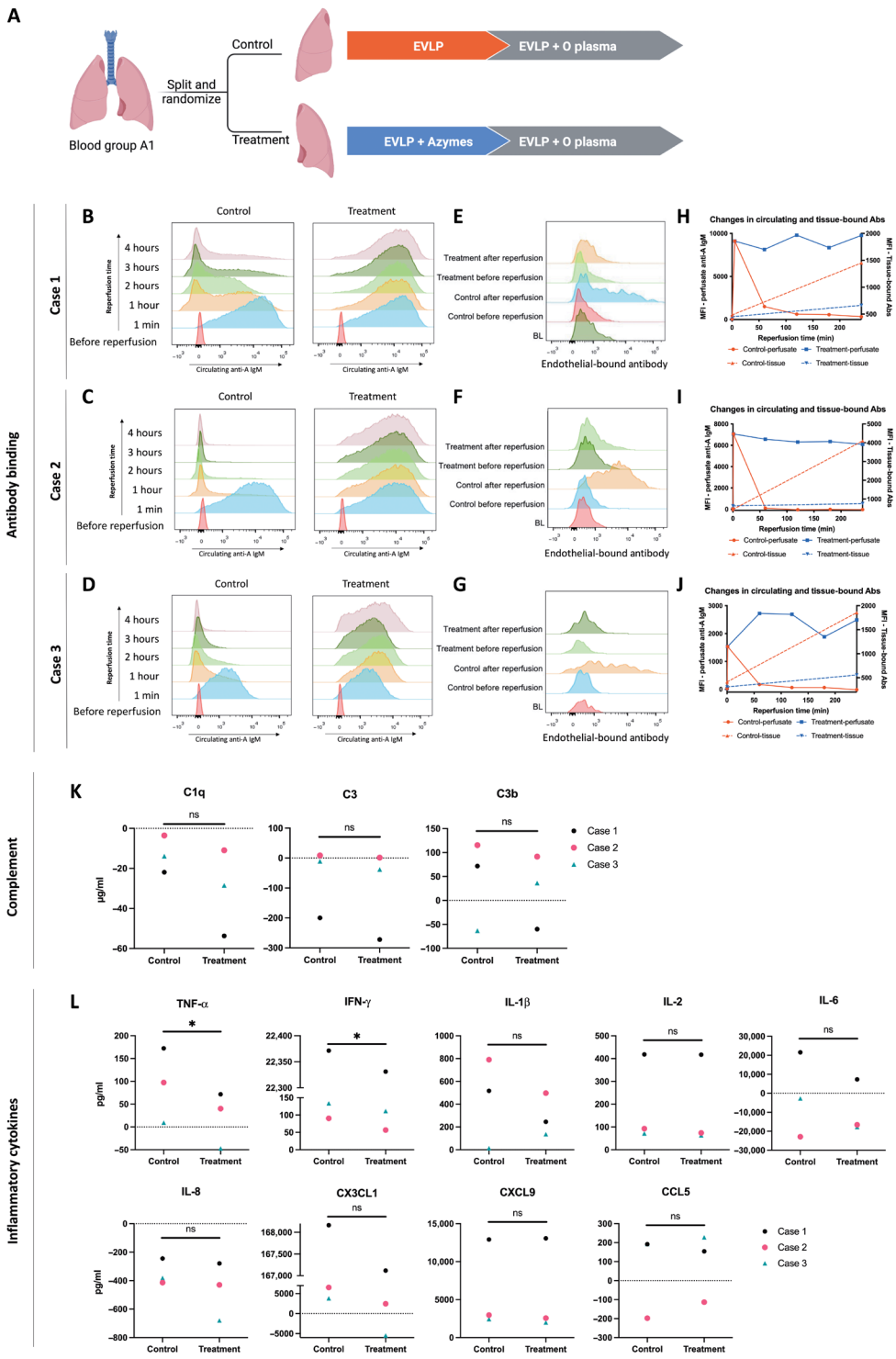

Fig. 4. Azyme treatment reduced evidence of rejection in an ex vivo simulation of ABOi lung transplant. An ABOi lung transplant simulation was used to determine effects of enzymatic preconditioning on antibody-mediated biological processes including antibody binding, complement activation, and inflammation. (**A**) A schematic shows the design of the ex vivo reperfusion model for ABOi lung transplantation. Lungs from same donor were separated to two distinct EVLP circuits and randomized into control (standard EVLP) or treatment (EVLP + enzyme) groups. ABO-O plasma was added to initiate reperfusion. (**B** to **J**) Antibody binding was measured over time after reperfusion. Antigen depletion in the treated lungs reduced antibody binding. (B to D) Histograms of anti-A antibodies in the perfusate sampled from the control and treatment groups before and after reperfusion are shown. (E to G) Histograms of antibody deposited on endothelial cells ($CD31^{+}CD45^{-}$) isolated from the lungs are shown. BL is the baseline, before lungs were perfused or treated. (H and I) MFIs of circulating anti-A IgM (left *y* axis) and tissue-bound antibodies (Abs) (right *y* axis) were quantified over time. (**K**) Complement deposition was compared between control and treatment groups. The concentration (μg/ml) shown on the graphs is the difference in the concentration of complement components in the perfusate before and 3 hours after reperfusion. Data were analyzed using paired *t* test. (**L**) Change in the concentration of TNF-α, IFN-γ, IL-1β, IL-2, IL-6, IL-8, CX3CL1, CXCL9, and CCL5 was measured in control lungs as compared with their treated counterparts. The concentration (pg/ml) shown is the difference in cytokine concentration in the perfusate before and 3 hours after reperfusion. Each pair of control and treatment lungs was from the same donor. Data were analyzed using paired *t* test. $^{*}P < 0.05$.

(*1*). In addition, for heart transplantation, the median U.S. waiting time is longest (13.8 months) for ABO-O candidates compared to ABO-A or ABO-B (5 months) and ABO-AB (2 months) patients (*12*). For kidney transplantation, the median U.S. waiting time for a deceased donor transplant is reported to be 4.9 years for ABO-B candidates, 4.4 years for ABO-O, 2.7 years for ABO-A, and 1.6 years for ABO-AB candidates (*13*). Clearly, the development of strategies to reduce transplant waiting lists by eliminating the need for ABO compatibility would be very attractive and would have a major impact in access to and fairness of organ allocation.

The use of glycolytic enzymes to cleave relevant carbohydrate epitopes from the surface of RBCs, thereby converting group A or B blood to "universal donor" group O, has been demonstrated previously (*7*). In 2009, Kobayashi *et al.* (*14*) intravenously administered an endo-galactosidase to baboons. However, the available enzymes were not specific or efficient enough to render this approach practical or safe on any substantial scale. The recent demonstration

Table 2. Profiles of donor A-Ag, cytokine expression, plasma antibody titers, and complement concentration before transplant simulations. Data were collected after treatment and before plasma reperfusion. IS, immediate spin; IAT, indirect antiglobulin test.

		Case 1		Case 2		Case 3	
		Control	Treatment	Control	Treatment	Control	Treatment
Donor A-Ag (MFI)		4,070	238	28,985	336	19,301	254
Donor baseline cytokine (pg/ml)	TNF-α	57.54	38.75	53.95	81.37	7.67	84.76
	IFN-γ	30.04	31.28	30.97	31.28	30.04	33.14
	IL-1β	321.79	433.92	37.25	50.23	62.14	162.56
	IL-2	34.52	36.10	35.05	36.10	33.21	36.62
	IL-6	24,966.80	40,027.96	89,036.49	79,242.31	44,794.32	54,351.42
	IL-8	3,562.10	3,638.00	3,499.50	3,572.60	3,687.30	3,780.20
	CX3CL1	4,886.35	5,932.83	5,944.38	5,049.87	20,810.40	25,254.29
	CXCL9	1,097.26	1,163.54	1,163.01	1,184.91	1,163.54	1,227.16
	CCL5	212.16	209.17	452.44	284.30	137.46	98.29
Plasma anti-A titers	IS (IgM)	16		16		8	
	IAT (IgG)	64		128		64	
Plasma complement (g/liter)	C3	0.785		0.599		0.913	
	C4	0.194		0.146		0.198	

by Rahfeld and co-workers (*8*) that the enzyme pair of FpGalNAc deacetylase and FpGalactosaminidase efficiently converts full units of ABO-A blood to ABO-O without the need for additional special conditions, together with the demonstration that the enzymes target all A-Ag subtypes with high specificity at both 4° and 37°C, suggests that they are ideally suited for donor organ modification.

In this study, we have demonstrated removal of histo-blood group A-Ag from ABO-A human lungs. Our whole-lung treatment was delivered during normothermic EVLP, a clinical technique that is now used routinely for lung preservation, assessment, and treatment. Using EVLP, donor lungs are maintained, perfused, and ventilated under physiological conditions for several hours before transplantation (*9*). This capability has allowed EVLP to be developed as a platform to deliver a variety of treatments to donor lungs before transplant, such as therapies to eliminate donor bacterial and viral infections, to decrease inflammation associated with brain death, and to treat thromboembolic events (*15*–*18*). This study further expands this capability into organ reengineering.

There are two main phenotypes of blood group A, the A1 and non-A1, which differ in antigenicity as determined by the amount of surface antigens (*19*). The surface of a subgroup A1 erythrocyte is reported to carry about 1 million blood group antigens, whereas a subgroup non-A1 erythrocyte displays less than one-third of that number (*3*). In our study, we also observed differing antigen intensity displayed on pulmonary cells from A1 versus non-A1 donors, with the average MFI of endothelial A-Ag from subgroup A1 donors being greater than 45 times compared with the MFI of subgroup non-A1 donors. Consequently, for our proof-of-concept lung study, we opted to use only lungs from A1 subgroup donors because this is the more challenging phenotype for ABOi transplants, thus providing a more stringent test of our treatment procedure than other A subgroups. Even so, we observed near-complete clearance of vascular A-Ag within 1 hour of treatment, making our approach attractive and likely readily translatable to clinical practice. Moreover, we show that practicality and scalability are not an issue, as whole-organ efficacy was achieved using an enzyme dose as low as 1 μg/ml (2 mg of each Azyme per double adult human lung EVLP, which uses 2 liters of perfusate solution). By comparison, the previous study using an endo-galactosidase required more than 10 mg of enzyme to treat baboons of pediatric size (*14*).

In the absence of any recipient desensitization or antibody removal protocol, the most critical phase for ABOi organ transplantation is the immediate posttransplant period when the naturally present (preformed) antibodies in the recipient attack foreign antigens on the donor graft, with high risk of rapid acute organ failure. Hyperacute rejection may be avoided if the antigens are removed first and subsequently do not rapidly regenerate. In our transplant simulation experiment, we demonstrated this concept by preconditioning donor lungs, thereby avoiding hyperacute damage from ABO-O plasma containing anti-A antibodies. As a direct result of Azyme-mediated antigen depletion, all three treated cases demonstrated effective inhibition of antibody binding and minimization of subsequent inflammatory responses (TNF-α and IFN-γ), which were observed in the control counterparts. Although the circulating complements C1q, C3, and C3b were not different between the treatment and control lungs, respectively, a pattern in tissue C4d deposition was observed, which may correlate with lung physiology. Although we only observed deterioration of lung physiology and positive tissue C4d deposition in two of the three control lungs, it is important to point out that our model uses plasma instead of whole blood. Antibody-mediated rejection is a complex process that involves multiple molecular and cellular processes to trigger physiological responses in an allograft (*20*). We initially focused our study on the cell-free compartment of blood to avoid cellular confounders. Reperfusion models with whole blood are thus a future direction. However, whole blood can be preserved up to only 21 days (*21*), and the time to recruit a pair of suitable lungs for study is inconsistent. Therefore, plasma was the most effective option for recipient

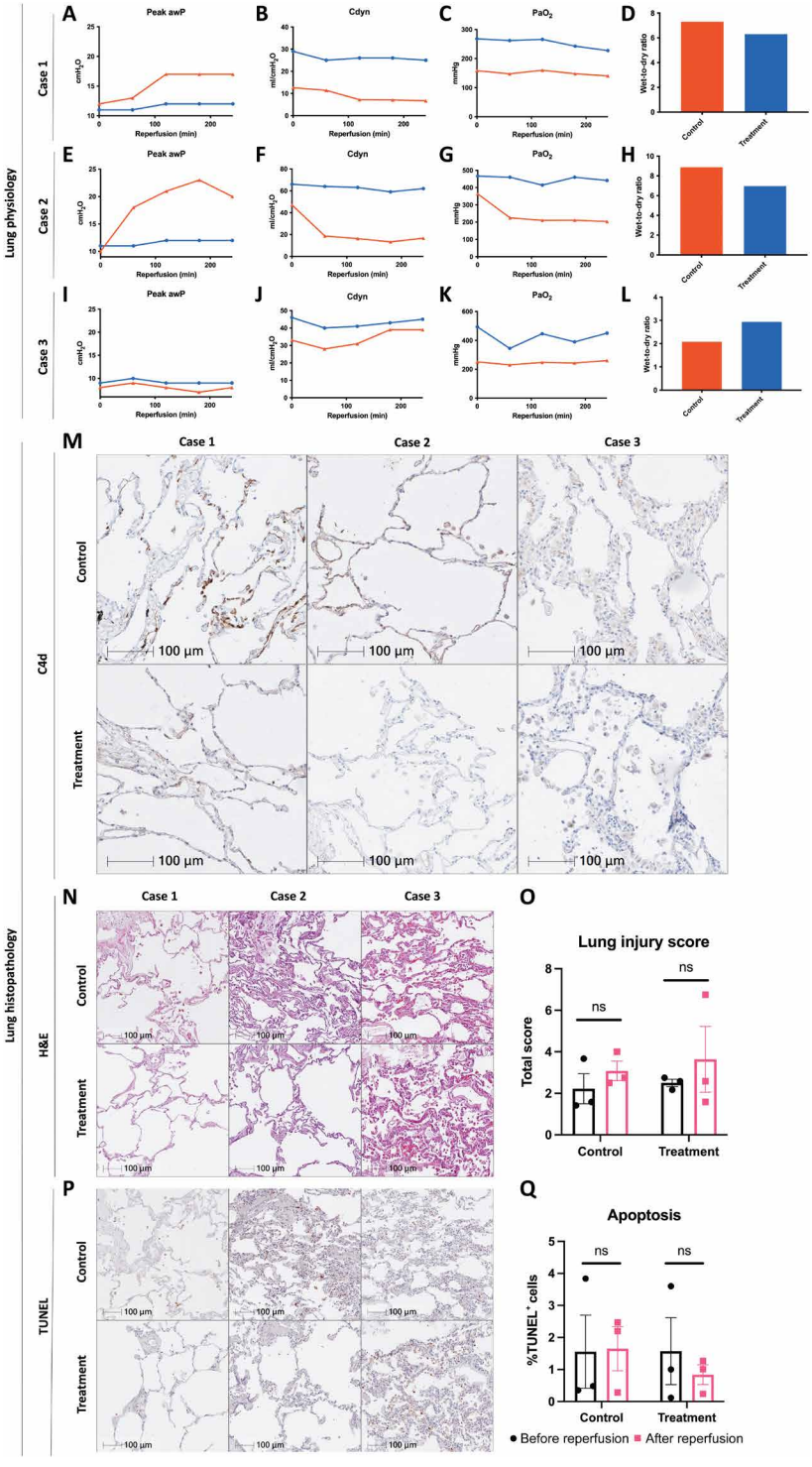

Fig. 5. Lung physiology and histopathology after reperfusion were modestly affected by Azyme treatment. (**A** to **L**) Lung physiology was evaluated for case 1 (A to D), case 2 (E to H), and case 3 (I to L). Peak airway pressure, dynamic compliance, arterial oxygen partial pressure (PaO_2), and estimation of lung edema based on wet-to-dry weight ratio of tissue sampled at the end of reperfusion are shown. The control lung is shown in red, and the treated lung is shown in blue. (**M** to **Q**) Lung histopathology after reperfusion was also evaluated. (M) Representative images show C4d staining of control and treatment after reperfusion. Grading from a blinded pathologist indicated that case 1–control sample was borderline positive (close to 50% capillary staining), case 2–control sample was positive (>50% capillary staining), and case 3–control sample was negative (<50% capillary staining); treated samples of all three cases were negative (<50% capillary staining). Scale bars, 100 μm. (N) Representative hematoxylin and eosin (H&E)–stained images of control and treated lungs after reperfusion are shown. Scale bars, 100 μm. (O) Lung injury scores were quantified before and after 4 hours of reperfusion. Data were analyzed by two-way ANOVA and Bonferroni's multiple comparisons test. (P) Representative TUNEL-stained images of control and treated lungs after reperfusion are shown. Scale bars, 100 μm. (Q) Apoptotic cells were quantified as a percentage of total cells before and after reperfusion. Data were analyzed by two-way ANOVA and Bonferroni's multiple comparisons test.

simulation. The inconsistent lung physiology and C4d staining observed in the control of case 3 could be due to either lower recipient anti-A antibody titer as compared with the other two cases or could be due to missing intermediate factors of the antibody-mediated rejection process in the plasma samples that were used.

One of the limitations of the study is the lack of information on antigen reexpression. From a mechanistic perspective, our treatment removes vascular A-Ag through a glycosidic pathway. Because the endogenous glycosyltransferases that install the ABH epitopes are still present, we recognize that organs will likely regenerate the cleaved A/B antigens. Although our transplant simulation studies show that the antigens do not regenerate for a few hours, studies to better understand the regeneration kinetics are warranted. However, the clinical relevance of that would be still questionable. In kidney ABOi transplantation, it is well described that despite recipient desensitization, eventually, anti-A antibodies reemerge. Oftentimes, complement C4d deposition is noted posttransplant in grafts of kidney ABOi recipients. However, this is typically not associated with graft dysfunction (*2*, *22*). Another limitation of the study is the absence of posttransplant clinical data. Although lung transplant models are available in animals such as pigs, the porcine blood group system is different from that of humans, making it difficult to translate findings from such animal models (*23*). The closest animal model that shares the same ABH system on tissue, as observed in human, is baboons (*24*). However, conducting research in such a model can be logistically complex. Recently, West and co-workers (*25*) developed a strain of blood group A transgenic mice that express A-Ag on endothelium and other tissue components. The authors also established a heart transplant antibody-mediated rejection model using this strain of mice. As next steps, we plan to use similar

transgenic mice to study antigen reexpression kinetics and long-term posttransplant effects of the organ donor enzymatic treatment.

In conclusion, our study shows that ex vivo enzymatic treatment of the donor lung can effectively remove A-Ag from ABO-A donor lungs without acute side effects. Organ antigen depletion prevented hyperacute antibody-mediated injuries in a simulation of lung transplantation. The treatment described here could potentially result in expansion of safe ABOi organ transplantation and further expand the pool of universal donor organs from the current 55% (blood group O donors) to over 80% with inclusion of modified A organs (based on Organ Procurement and Transplantation Network data as of 30 November 2021). As a consequence, this strategy may greatly improve access and fairness of organ allocation.

MATERIALS AND METHODS

Study design

The goal of this study was to explore feasibility and safety of using the Azymes to remove A-Ag from donor lungs during EVLP. The Azymes' antigen removal effects were systematically examined on the cellular level with ABO-A1 human RBCs (n = 5 per group), on the tissue level with human aortae (n = 3 per group), and on the whole-organ level with EVLP lungs (nine lungs were treated as shown in Table 1, but only eight lungs provided cell samples for flow cytometric analyses). We also studied the effects of A-Ag depletion on preventing antibody-mediated injury using a model that simulated reperfusion of an ABOi lung transplant (n = 3 per group). For the in vitro and ex vivo studies, the number of replicates was determined on the basis of previous experience and organ availability. In the paired lung studies, the left and right lungs were assigned randomly to experimental and control groups by an independent member outside the research team without prior knowledge of lung quality. The investigator conducting the histological gradings was blinded to treatment allocation.

Human specimens

Protocols involving the use of human specimens (RBCs, tissues, and organs) were approved by the institutional research ethics board of the University Health Network and the organ donation organization Trillium Gift of Life Network. Informed research consent was obtained. The use of plasma samples was approved by the institutional research ethics board of the University Health Network and the Canadian Blood Services, and samples were obtained through the Blood4Research Program from the Canadian Blood Services.

Materials

The lung perfusate solution used in the study is STEEN solution (XVIVO Perfusion), same as those used in the Toronto EVLP protocol. Azymes (FpGalNAc deacetylase and FpGalactosaminidase) were expressed according to published protocol (*8*). Briefly, the proteins were cloned into pET16b or pET28a vectors. Production of proteins was performed in BL21(DE3) cells, cultured in ZY5052 auto induction medium (20 hours at 37°C, 220 rpm), and inoculated with overnight LB culture. Then, cells were collected by centrifugation and lysed with a lysis buffer on ice. Cell debris was removed by centrifugation, and cell lysate was collected. Purification was conducted through a nickel affinity chromatography column and a hydrophobic interaction chromatography column, followed by an endotoxin reduction step (Pierce High-Capacity Endotoxin Removal Resin). The purified enzymes were identified by SDS–polyacrylamide gel electrophoresis. Confirmed proteins were formulated in PBS (pH 7.4) at a concentration of 2 mg/ml. Aliquots of 1 ml were prepared and stored at −80°C until use.

RBC treatment

ABO-A1 whole blood was collected into citrate Vacutainer (363083, BD Biosciences) from consented organ donors. The tubes were centrifuged at 1000*g* at room temperature for 5 min, and RBCs were separated and washed three times with PBS containing 0.2% bovine serum albumin. Washed RBCs were prepared as a 1% hematocrit solution and treated with Azyme-spiked perfusate solution at 37°C (n = 5). PBS at 37°C, the previously reported solution used for RBC treatment (*8*), was used as a comparison group. The temperature chosen for perfusate solution was based on its working temperature in clinical practice (*9*). After Azyme treatment, RBCs were incubated in cell staining buffer (420201, BioLegend) at 4°C for 30 min with mouse anti-human blood group A monoclonal antibody (MA19693, Invitrogen), followed by incubation at 4°C for 30 min with FITC-labeled goat anti-mouse immunoglobulin M (IgM) (31992, Invitrogen). The antibodies were diluted to 1:25. Flow cytometry data were acquired on an LSR II (BD Biosciences). The degree of antigen removal was analyzed using FlowJo v10 (FlowJo LLC) and quantified as %Antigen Removal = [MFI(A_RBC) − MFI(A_RBC + Azymes)]/[MFI(A_RBC) − MFI(O_RBC)]*100%. A dose-escalation study was carried out to help predict the appropriate dose to be used in organs. The unit of dose used throughout the study is defined as weight of enzymes (microgram) over volume of solution (milliliter).

Aorta treatment

To test the ability of Azymes to remove A-Ag from tissue, an in vitro model of a human artery was used. From each human donor (ABO-A1), the aorta (n = 3 per group) was split into control (perfusate solution) and treatment (enzyme-spiked perfusate solution) groups and incubated statically at 37°C for 4 hours (21% O_2 and 5% CO_2). Biopsies were taken at the end of incubation for both groups, and expression of A-Ag was analyzed by immunohistochemistry. Detailed methods to immunohistochemistry are described in the immunohistochemistry section below. Briefly, consecutive 5-μm sections of the biopsies were stained with rabbit anti-CD31 antibody (ab28364, Abcam), a marker of endothelial cells diluted to 1:100, and anti-A antibody (MA19693, Invitrogen) diluted to 1:200 to show the location and expression of A-Ag. Whole slides were scanned using a slide scanner (Aperio CS2, Leica). The scanned images of the whole slides were used for analyses by HALO Image Analysis Software (Indica Labs). The A-Ag–positive areas were calculated using the Area Quantification algorithm of HALO. The degree of A-Ag–positive area in the treated tissue was normalized against the untreated tissue and adjusted by the total tissue area: % Normalized A-Ag = (Area_Aag(treatment)/Area_Aag(control))*(Area_tissue(treatment)/Area_tissue(control))*100%.

Immunohistochemistry

Formalin-fixed paraffin-embedded (FFPE) tissue samples were sectioned into 5 μm using a rotary microtome (Microm HM325, Thermo Scientific), followed by deparaffination in xylene and rehydration through graded ethanol. Peroxidase activity was blocked by 3% H_2O_2; heat-induced epitope retrieval was achieved using

citrate buffer (ab93678, Abcam), and nonspecific protein binding was blocked using serum-free protein block (X0909, Dako-Agilent). To detect endothelial cells, tissue sections were stained with 1:100 rabbit anti-human CD31 antibody (28364, Abcam), followed by biotinylated anti-rabbit Ig (BA-1000, Vector Labs). To detect blood group antigens, tissue sections were stained with 1:200 mouse anti-human A-Ag antibody (MA1-19693, Thermo Fisher) or 1:100 mouse anti-human H-Ag antibody (sc-59467, Santa Cruz Biotechnology), followed by biotinylated anti-mouse antibody (BA-2000, Vector Labs). Immunostaining was achieved by an avidin-biotin complex (ABC) kit (PK-6100, Vector Labs), followed by 3,3′-diaminobenzidine (DAB) (ab64238, Abcam) for brown color or 3-amino-9-ehtylcarbazole (AEC) (K3464, Agilent) for red color. Slides were counterstained with Harris' hematoxylin (RC353032, VWR) or Mayer's hematoxylin (MHS1, Sigma-Aldrich), respectively. Whole slides were scanned using slide scanner (Aperio CS2, Leica) for subsequent image analyses.

Flow cytometry

Lung tissues were processed into single-cell suspensions according to a previously published protocol (*26*). Briefly, fresh lung tissues were digested with collagenase D and deoxyribonuclease I (STEMCELL Technologies) using a gentleMACS tissue dissociator (Miltenyi Biotec). For antigen expression, cells were stained with LIVE/DEAD marker Aqua fixable viability dye (423103, BioLegend) in 1:1000 dilution at room temperature, followed by blocking with Fc Block (564220, BD Biosciences) at 4°C for 10 min and staining with a cocktail of fluorochrome-conjugated monoclonal antibodies in cell staining buffer (420201, BioLegend) at 4°C for 30 min. Details of the antibodies and dilutions used were summarized in table S1. After staining, cells were fixed with fixation buffer (420801, BioLegend). For antibody deposition, cells were incubated with FITC-conjugated anti-human IgM first (4°C, 30 min), washed with cell staining buffer (420201, BioLegend), blocked with Fc Block (564220, BD Biosciences), and then stained with the remaining panel of fluorochrome-conjugated monoclonal antibodies (table S1) and Zombie Aqua fixable viability dye (423103, BioLegend). After staining, cells were fixed with fixation buffer (420801, BioLegend). For measurement of perfusate anti-A antibodies, 100 μl of perfusates was incubated with 50 μl of reference A1 RBC (2345, Immucor Inc.) at 37°C for 30 min. Cells were washed with cell staining buffer and subsequently stained with FITC-conjugated anti-human IgM (31575, Invitrogen). All flow cytometry data were acquired on an LSR II (BD Biosciences) and analyzed using FlowJo v10 (FlowJo LLC).

EVLP protocol

Unless otherwise stated, all EVLP performed in this study followed the established Toronto EVLP protocol (*27*). Briefly, heart-lung blocks from donors were flushed antegrade with 3 liters of low potassium dextran solution during organ retrieval, followed by 1 liter of retrograde flush after cannulation of pulmonary artery and left atrium and placement of endotracheal tube upon arrival at the receiving hospital. The organ was placed on an XVIVO organ chamber (XVIVO), the endotracheal tube was connected to an intensive care unit ventilator, and the cannulas were connected to the perfusion circuit. A cell-free albumin perfusate solution, STEEN solution (XVIVO), was used in a quantity of 1.5 liters for single lung and 2 liters for double lungs. Additives, including 3000 IU of sodium heparin (Leo Pharma Inc.), 500 mg of methylprednisolone (Pfizer), and 500 mg of imipenem (Primaxin; Merck), were added to the perfusate before perfusion was started. The lungs were perfused at a target flow of 40% of the predicted cardiac output of the donor. The temperature of perfusate was gradually increased to 37°C; volume-controlled ventilation was initiated when perfusate temperature reached 32°C. Hourly assessment was performed for lung physiology, including airway pressure, lung compliance, vascular resistance, and perfusate blood gas analysis.

Ex vivo treatment of perfused human lungs

The efficacy of enzyme-containing EVLP in removing histo-blood group antigens was studied in human lungs. Donor lungs, determined as nonsuitable for transplantation, were used. If lungs were declined for use in transplantation while already on clinical EVLP, enzymes were added to the perfusion liquid to initiate treatment. If lungs were declined for transplant at the donor hospital before EVLP, EVLP was set up per standard protocol. Azymes were added to the perfusate solution after hour 1 assessment when full flow was achieved. Lungs were perfused and assessed following the standard Toronto EVLP protocol; biopsies were taken before and after treatment. The expression of histo-blood group antigens was analyzed by immunohistochemistry and flow cytometry as described above. Lung physiology (peak airway pressure, dynamic compliance, pulmonary vascular resistance, and perfusate blood gas) and inflammatory cytokines [including interleukin-6 (IL-6), IL-8, IL-1β, IL-2, TNF-α, and IFN-γ] were assessed for potential acute adverse side effects of enzyme treatment.

Ex vivo ABOi transplant simulation model

ABO-A1 human lungs declined for transplantation were used as donors, and ABO-O plasma samples were used as recipients. The anti-A antibody titers and complement (C3 and C4) of the ABO-O plasma were tested at the Laboratory Medicine Program (University Health Network) following standard protocols to ensure the presence of antibody and complement. Upon arrival, lungs were split into two blocks, placed into two independent EVLP circuits, and randomized into control (EVLP) and treatment (EVLP + enzyme) groups. Lungs were perfused using the Toronto EVLP protocol (*27*). Azymes were added to the treatment lung after hour 1 assessment, when full flow and ventilation had been achieved. After 1 to 3 hours of treatment at full flow, 3 units of ABO-O plasma (about 900 ml) was added to each group to simulate "posttransplant" antibody responses. Lungs were subsequently observed for 4 hours (the reperfusion period), during which physiologic parameters, including airway pressures, pulmonary compliance, and perfusate blood gas, were evaluated hourly. Biopsies were taken before EVLP, before adding ABO-O plasma, and at the end of reperfusion. Antibody deposition on lung tissue was analyzed by flow cytometry. Anti-A antibodies in perfusate at defined time points throughout reperfusion were measured using reagent RBC reference A1 cells (2345, Immucor Inc.) and analyzed by flow cytometry. The total anti-A antibody introduced by the plasma was denoted as the 1-min time point for both control and treatment and was measured from recipient plasma diluted according to the actual dilution factor: For example, if 900 ml of plasma was added to a circuit primed with 1.5 liters of perfusate solution, plasma was diluted by the dilution factor of 0.38 and subjected to anti-A antibody measurement. Perfusate complements (C1q, C3, and C3b) and inflammatory cytokines (TNF-α, IFN-γ, IL-1β, IL-2, IL-6, IL-8, CX3CL1, CXCL9, and CCL5) before and

after reperfusion were also assessed. Histopathological assessment of reperfusion injury was assessed on the basis of C4d deposition, lung injury scores, and TUNEL staining. Details are described below.

EVLP sample collection protocol

Perfusate and tissue samples were collected before treatment, after treatment, and after reperfusion in the case of ABOi transplant simulation unless otherwise stated. Lung tissue was sampled from lower lobe at baseline, and tissue was sampled from multiple locations (upper and lower lobes for left lung and upper, middle, and lower lobes from right lung) at the end of treatment and reperfusion studies. Lung tissues were divided into three parts: One part was freshly homogenized into single-cell suspension, stored in freezing media (fetal calf serum plus 5% dimethyl sulfoxide), and preserved in liquid nitrogen for flow cytometric analyses; one part was snap frozen and stored at −80°C for cytokine studies; and one part was fixed with 10% phosphate-buffered formalin for 24 hours and then embedded in paraffin for histological analysis. For the reperfusion study, an additional tissue sample was collected at the end of reperfusion for wet-to-dry weight ratio analysis to estimate lung edema.

Analysis of C4d deposition

Sections (5 μm) of FFPE lung tissues were stained at the Laboratory Medicine Program (University Health Network) with a standard C4d staining protocol. C4d staining was assessed by a pulmonary pathologist in a blinded fashion. Samples were graded as follows: positive (>50% alveolar capillary staining by C4d) and negative (<50% alveolar capillary staining by C4d) (*28*).

Acute lung injury scoring

Sections (5 μm) of FFPE lung tissues were stained with a standard hematoxylin and eosin staining protocol. Acute lung injury scores were assessed by a pulmonary pathologist in a blinded fashion using the following parameters: air space hemorrhage, vascular congestion, edema/fibrin in the alveoli, and infiltration of white blood cells. The severity of these parameters was graded from 0 to 3 as follows: 0 (absent), 1 (mild), 2 (moderate), and 3 (severe) (*29*). Total scores were reported.

Analysis of tissue apoptosis

Sections (5 μm) of FFPE lung tissues were stained with TUNEL. Terminal transferase (03333566001, Roche) and biotin-16-dUTP (11093070910, Roche) were prepared according to the manufacturer's instruction. Slides were stained red using AEC substrate and counterstained with Mayer's hematoxylin. TUNEL-stained slides were scanned and analyzed using the CytoNuclear algorithm of the HALO Image Analysis Software (Indica Labs). The degree of apoptosis was calculated and normalized on the basis of the percentage of $TUNEL^+$ cells over total number of cells.

Complement assay and inflammatory cytokine assay

Perfusates were assayed for complement components using the Multiplex Human Complement Panel 2 (C1q, C3, and C3b) from Millipore (HCMP2MAG-19K) according to the manufacturer's instructions. Perfusates were assayed for cytokines using a human multiplex panel (TNF-α, IL-6, IL-8, IL-1β, IL-2, IFN-γ, CX3CL1, CCL5, and CXCL9) from R&D Systems according to the manufacturer's instructions. Data were acquired with a Luminex MAGPIX instrument and analyzed using xPONENT software (Bio-Techne).

Statistical analysis

The data, where relevant, are from at least three independent experiments of biological replicates. All statistical details can be found in the figures and figure legends. All experimental results are expressed as means ± SEM unless stated otherwise. For the paired lung studies, paired *t* test was performed to compare differences between groups. For comparisons between multiple groups, Kruskal-Wallis tests followed by Dunn's multiple comparisons tests were performed. For data involving a second component, a two-way analysis of variance (ANOVA) was used followed by a Bonferroni's correction for multiple comparisons unless stated otherwise. All analyses were conducted using GraphPad Prism 9.0 software (GraphPad Software). Statistical significance was defined as $P < 0.05$.

SUPPLEMENTARY MATERIALS

www.science.org/doi/10.1126/scitranslmed.abm7190
Figs. S1 to S5
Table S1
Data file S1
MDAR Reproducibility Checklist

View/request a protocol for this paper from *Bio-protocol*.

REFERENCES AND NOTES

1. Y. D. Barac, M. S. Mulvihill, M. L. Cox, M. Bishawi, J. Klapper, J. Haney, M. Daneshmand, M. G. Hartwig, Implications of blood group on lung transplantation rates: A propensity-matched registry analysis. *J. Heart Lung Transplant.* **38**, 73–82 (2019).
2. C. Morath, M. Zeier, B. Döhler, G. Opelz, C. Süsal, ABO-incompatible kidney transplantation. *Front. Immunol.* **8**, 234 (2017).
3. K. Takahashi, A new concept of accommodation in ABO-incompatible kidney transplantation. *Clin. Transpl.* **19** Suppl 14, 76–85 (2005).
4. M. Garcia de Mattos Barbosa, M. Cascalho, J. L. Platt, Accommodation in ABO-incompatible organ transplants. *Xenotransplantation* **25**, e12418 (2018).
5. F. G. Scurt, L. Ewert, P. R. Mertens, H. Haller, B. M. W. Schmidt, C. Chatzikyrkou, Clinical outcomes after ABO-incompatible renal transplantation: A systematic review and meta-analysis. *Lancet* **393**, 2059–2072 (2019).
6. A. E. de Weerd, M. G. H. Betjes, ABO-incompatible kidney transplant outcomes: A meta-analysis. *Clin. J. Am. Soc. Nephrol.* **13**, 1234–1243 (2018).
7. Q. P. Liu, G. Sulzenbacher, H. Yuan, E. P. Bennett, G. Pietz, K. Saunders, J. Spence, E. Nudelman, S. B. Levery, T. White, J. M. Neveu, W. S. Lane, Y. Bourne, M. L. Olsson, B. Henrissat, H. Clausen, Bacterial glycosidases for the production of universal red blood cells. *Nat. Biotechnol.* **25**, 454–464 (2007).
8. P. Rahfeld, L. Sim, H. Moon, I. Constantinescu, C. Morgan-Lang, S. J. Hallam, J. N. Kizhakkedathu, S. G. Withers, An enzymatic pathway in the human gut microbiome that converts A to universal O type blood. *Nat. Microbiol.* **4**, 1475–1485 (2019).
9. M. Cypel, J. C. Yeung, M. Liu, M. Anraku, F. Chen, W. Karolak, M. Sato, J. Laratta, S. Azad, M. Madonik, C.-W. Chow, C. Chaparro, M. Hutcheon, L. G. Singer, A. S. Slutsky, K. Yasufuku, M. de Perrot, A. F. Pierre, T. K. Waddell, S. Keshavjee, Normothermic ex vivo lung perfusion in clinical lung transplantation. *N. Engl. J. Med.* **364**, 1431–1440 (2011).
10. R. Chapanian, D. H. Kwan, I. Constantinescu, F. A. Shaikh, N. A. A. Rossi, S. G. Withers, J. N. Kizhakkedathu, Enhancement of biological reactions on cell surfaces via macromolecular crowding. *Nat. Commun.* **5**, 4683 (2014).
11. M. Senior, Beating the organ clock. *Nat. Biotechnol.* **36**, 488–492 (2018).
12. M. Colvin, J. M. Smith, N. Hadley, M. A. Skeans, K. Uccellini, R. Lehman, A. M. Robinson, A. K. Israni, J. J. Snyder, B. L. Kasiske, OPTN/SRTR 2017 annual data report: Heart. *Am. J. Transplant.* **19**, 323–403 (2019).
13. W. W. Williams, W. S. Cherikh, C. J. Young, P. Y. Fan, Y. Cheng, D. A. Distant, C. F. Bryan, First report on the OPTN national variance: Allocation of A2 /A2 B deceased donor kidneys to blood group B increases minority transplantation. *Am. J. Transplant.* **15**, 3134–3142 (2015).
14. T. Kobayashi, D. Liu, H. Ogawa, Y. Miwa, T. Nagasaka, S. Maruyama, Y.-T. Li, A. Onishi, M. Iwamoto, T. Kuzuya, K. Kadomatsu, K. Uchida, A. Nakao, Removal of blood group A/B antigen in organs by ex vivo and in vivo administration of endo-ß-galactosidase (ABase) for ABO-incompatible transplantation. *Transpl. Immunol.* **20**, 132–138 (2009).
15. M. Cypel, J. J. Feld, M. Galasso, R. V. Pinto Ribeiro, N. Marks, M. Kuczynski, D. Kumar, I. Bahinskaya, V. S. Bagnato, C. Kurachi, A. S. Slutsky, J. C. Yeung, L. Donahoe, M. de Perrot, K. Yasufuku, A. Pierre, M. Binnie, C. Chaparro, T. Martinu, M. Chen, J. Tikkanen, C.-W. Chow, A. Sidhu, T. K. Waddell, S. Keshavjee, L. G. Singer, A. Humar, Prevention

of viral transmission during lung transplantation with hepatitis C-viraemic donors: An open-label, single-centre, pilot trial. *Lancet Respir. Med.* **8**, 192–201 (2020).
16. M. Galasso, J. J. Feld, Y. Watanabe, M. Pipkin, C. Summers, A. Ali, R. Qaqish, M. Chen, R. V. P. Ribeiro, K. Ramadan, L. Pires, V. S. Bagnato, C. Kurachi, V. Cherepanov, G. Moonen, A. Gazzalle, T. K. Waddell, M. Liu, S. Keshavjee, B. C. Wilson, A. Humar, M. Cypel, Inactivating hepatitis C virus in donor lungs using light therapies during normothermic ex vivo lung perfusion. *Nat. Commun.* **10**, 481–412 (2019).
17. J. C. Yeung, D. Wagnetz, M. Cypel, M. Rubacha, T. Koike, Y.-M. Chun, J. Hu, T. K. Waddell, D. M. Hwang, M. Liu, S. Keshavjee, Ex vivo adenoviral vector gene delivery results in decreased vector-associated inflammation pre- and post-lung transplantation in the pig. *Mol. Ther.* **20**, 1204–1211 (2012).
18. M. Cypel, M. Liu, M. Rubacha, J. C. Yeung, S. Hirayama, M. Anraku, M. Sato, J. Medin, B. L. Davidson, M. de Perrot, T. K. Waddell, A. S. Slutsky, S. Keshavjee, Functional repair of human donor lungs by IL-10 gene therapy. *Sci. Transl. Med.* **1**, 4ra9 (2009).
19. M. E. Breimer, J. Mölne, G. Nordén, L. Rydberg, G. Thiel, C. T. Svalander, Blood group A and B antigen expression in human kidneys correlated to A1/A2/B, Lewis, and secretor status. *Transplantation* **82**, 479–485 (2006).
20. N. M. Valenzuela, E. F. Reed, Antibody-mediated rejection across solid organ transplants: Manifestations, mechanisms, and therapies. *J. Clin. Invest.* **127**, 2492–2504 (2017).
21. H. F. Pidcoke, S. J. McFaul, A. K. Ramasubramanian, B. K. Parida, A. G. Mora, C. G. Fedyk, K. K. Valdez-Delgado, R. K. Montgomery, K. M. Reddoch, A. C. Rodriguez, J. K. Aden, J. A. Jones, R. S. Bryant, M. R. Scherer, H. L. Reddy, R. P. Goodrich, A. P. Cap, Primary hemostatic capacity of whole blood: A comprehensive analysis of pathogen reduction and refrigeration effects over time. *Transfusion* **53** Suppl 1, 137S–149S (2013).
22. G. A. Böhmig, A. M. Farkas, F. Eskandary, T. Wekerle, Strategies to overcome the ABO barrier in kidney transplantation. *Nat. Rev. Nephrol.* **11**, 732–747 (2015).
23. D. M. Smith, M. Newhouse, B. Naziruddin, L. Kresie, Blood groups and transfusions in pigs. *Xenotransplantation* **13**, 186–194 (2006).
24. R. Oriol, J. Le Pendu, R. Mollicone, Genetics of ABO, H, Lewis, X and related antigens. *Vox Sang.* **51**, 161–171 (1986).
25. B. Motyka, N. Fisicaro, S.-I. Wang, A. Kratochvil, K. Labonte, K. Tao, J. Pearcey, T. Marshall, M. Mengel, B. Sis, X. Fan, A. J. F. d'Apice, P. J. Cowan, L. J. West, Antibody-mediated rejection in a blood group A-transgenic mouse model of ABO-incompatible heart transplantation. *Transplantation* **100**, 1228–1237 (2016).
26. T. Watanabe, T. Martinu, A. Chruscinski, K. Boonstra, B. Joe, M. Horie, Z. Guan, K. F. Bei, D. M. Hwang, M. Liu, S. Keshavjee, S. C. Juvet, A B cell-dependent pathway drives chronic lung allograft rejection after ischemia-reperfusion injury in mice. *Am. J. Transplant.* **19**, 3377–3389 (2019).
27. M. Cypel, J. C. Yeung, S. Hirayama, M. Rubacha, S. Fischer, M. Anraku, M. Sato, S. Harwood, A. Pierre, T. K. Waddell, M. de Perrot, M. Liu, S. Keshavjee, Technique for prolonged normothermic ex vivo lung perfusion. *J. Heart Lung Transplant.* **27**, 1319–1325 (2008).
28. G. Berry, M. Burke, C. Andersen, A. Angelini, P. Bruneval, F. Calabrese, F. Calbrese, M. C. Fishbein, M. Goddard, O. Leone, J. Maleszewski, C. Marboe, D. Miller, D. Neil, R. Padera, D. Rassl, D. Rassi, M. Revello, A. Rice, S. Stewart, S. A. Yousem, Pathology of pulmonary antibody-mediated rejection: 2012 update from the Pathology Council of the ISHLT. *J. Heart Lung Transplant.* **32**, 14–21 (2013).
29. M. Cypel, M. Rubacha, J. Yeung, S. Hirayama, K. Torbicki, M. Madonik, S. Fischer, D. Hwang, A. Pierre, T. K. Waddell, M. de Perrot, M. Liu, S. Keshavjee, Normothermic ex vivo perfusion prevents lung injury compared to extended cold preservation for transplantation. *Am. J. Transplant.* **9**, 2262–2269 (2009).
30. A. Varki, R. D. Cummings, M. Aebi, N. H. Packer, P. H. Seeberger, J. D. Esko, P. Stanley, G. Hart, A. Darvill, T. Kinoshita, J. J. Prestegard, R. L. Schnaar, H. H. Freeze, J. D. Marth, C. R. Bertozzi, M. E. Etzler, M. Frank, J. F. Vliegenthart, T. Lütteke, S. Perez, E. Bolton, P. Rudd, J. Paulson, M. Kanehisa, P. Toukach, K. F. Aoki-Kinoshita, A. Dell, H. Narimatsu, W. York, N. Taniguchi, S. Kornfeld, Symbol nomenclature for graphical representations of glycans. *Glycobiology* **25**, 1323–1324 (2015).

Acknowledgments: We thank P. Chartrand for supplies and logistics management, and H. Shan, M. Chen, C. Yang, B. Gomes, M. Galasso, T. Ku, and O. Hough for support. **Funding:** This work was funded by the University Health Network Foundation (to M.C.), the Collaborative Health Research Project funds from the Canadian Institute of Health Research and the Natural Sciences and Engineering Research Council (no. 433417; to M.C., L.W., and S.G.W.), and the Toronto General Hospital Research Institute PDF Award (to A.W.). **Author contributions:** A.W., R.V.P.R., A.A., E.B., E.A.-B., V.M., Y.Z., P.R., H.M., H.G. and P.P. participated in data acquisition and model development. P.R. and H.M. expressed the Azymes used in the study. A.W. performed the in vitro experiments. A.W., R.V.P.R., A.A., E.B., E.A.-B., H.G., and V.M. performed the ex vivo experiments. Y.Z. performed the immunohistochemistry staining. A.W. and R.V.P.R. performed the multiplex assays. P.P. did the blinded histological scorings. A.G. and V.M. provided operational assistance. A.W., M.L., T.K.W., C.C.-G., K.T., J.N.K., L.W., S.K., S.G.W., and M.C. were involved in the conception and experimental design of the study. A.W. and M.C. wrote and prepared the manuscript with input from all authors. M.C. was the study supervisor. **Competing interests:** M.C., T.K.W., and S.K. are shareholders of Traferox Inc. and consultants for Lung Bioengineering Inc. S.G.W., J.N.K., H.M., and P.R. are founders of ABOzymes Biomedical Inc., which is commercializing the enzymes described. A.W., M.C., S.K., J.N.K., P.R., and S.G.W. are inventors on patent application (PCT no. WO2020034043A1) submitted by the University of British Columbia and the University Health Network that pertains to the results presented in the paper. **Data and materials availability:** All data associated with this study are present in the paper or the Supplementary Materials. Enzymes (FpGalNAc deacetylase and FpGalactosaminidase) were provided from S.G.W. under a material transfer agreement with the University of British Columbia (UBC). UBC is in the process of licensing the IP for the enzymes to the company ABOzymes.

Submitted 6 October 2021
Accepted 22 December 2021
Published 16 February 2022
10.1126/scitranslmed.abm7190

Science Translational Medicine

Ex vivo enzymatic treatment converts blood type A donor lungs into universal blood type lungs

Aizhou WangRafaela V. P. RibeiroAadil AliEdson BrambateEtienne Abdelnour-BerchtoldVinicius MichaelsenYu ZhangPeter RahfeldHaisle MoonHemant GokhaleAnajara GazzalleProdipto PalMingyao LiuThomas K. WaddellChristine Cserti-GazdewichKathryn TinckamJayachandran N. KizhakkedathuLori WestShaf KeshavjeeStephen G. WithersMarcelo Cypel

Sci. Transl. Med., 14 (632), eabm7190.

Improving organ allocation in transplant

A major challenge in lung transplantation is the need for ABO blood group matching. To address this challenge, Wang *et al.* used two enzymes, FpGalNAc deacetylase and FpGalactosaminidase, to convert blood group A lungs to blood group O lungs during ex vivo lung perfusion. The authors demonstrated successful removal of blood group A antigen with no overt changes in lung health. In an ex vivo simulation of transplantation, the authors showed reduced antibody and complement deposition, suggesting that this technique may reduce antibody-mediated injury in vivo. Together, these findings have the potential to improve fairness in lung allocation for transplantation.